



HAL
open science

Zirconocene-Catalyzed Polymerization of alpha-Olefins: When Intrinsic Higher Activity Is Flawed by Rapid Deactivation

Xavier Desert, Fabien Proutiere, Alexandre Welle, Katty den Dauw, Aurelien Vantornme, Olivier Miserque, Jean-Michel Brusson, Jean-Francois Carpentier, Evgueni Kirillov

► **To cite this version:**

Xavier Desert, Fabien Proutiere, Alexandre Welle, Katty den Dauw, Aurelien Vantornme, et al.. Zirconocene-Catalyzed Polymerization of alpha-Olefins: When Intrinsic Higher Activity Is Flawed by Rapid Deactivation. *Organometallics*, 2019, 38 (13), pp.2664-2673. 10.1021/acs.organomet.9b00253 . hal-02278426

HAL Id: hal-02278426

<https://univ-rennes.hal.science/hal-02278426>

Submitted on 23 Sep 2019

HAL is a multi-disciplinary open access archive for the deposit and dissemination of scientific research documents, whether they are published or not. The documents may come from teaching and research institutions in France or abroad, or from public or private research centers.

L'archive ouverte pluridisciplinaire **HAL**, est destinée au dépôt et à la diffusion de documents scientifiques de niveau recherche, publiés ou non, émanant des établissements d'enseignement et de recherche français ou étrangers, des laboratoires publics ou privés.

Zirconocene-Catalyzed Polymerization of α -Olefins: When Intrinsic Higher Activity is Flawed by Rapid Deactivation

Xavier Desert,^{a,†} Fabien Proutiere,^{a,†} Alexandre Welle,^b Katty Den Dauw,^b Aurélien Vantomme,^b
Olivier Miserque,^b Jean-Michel Brusson,^c Jean-François Carpentier^{a,†*} and Evgueni Kirillov^{a,†*}

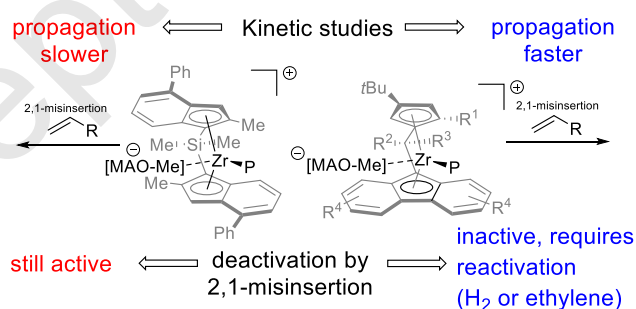
^a Univ Rennes, CNRS, ISCR (Institut des Sciences Chimiques de Rennes), UMR 6226, F-35700
Rennes, France

^b Total Research & Technology Feluy, Zone Industrielle Feluy C, B-7181 Seneffe, Belgium

^c Total S.A., Direction R&D Groupe, Tour Michelet A, 24 Cours Michelet – La Défense 10, F-92069
Paris La Défense Cedex, France

Dedicated to Prof. Mikhail Bochkarev on the occasion of his 80th birthday

Graphical Abstract / For the Table of content entry



[†] Those two authors equally contributed to this work.

* Correspondence to Jean-François Carpentier (jean-francois.carpentier@univ-rennes1.fr) and Evgueni Kirillov (evgueni.kirillov@univ-rennes1.fr); Fax: +33 (0)223236938.

ABSTRACT

Kinetic studies of homogeneous 1-hexene polymerization have been used for determining the propagation rates and active sites concentrations of industrially-relevant zirconocene catalytic systems incorporating {SBI}- and {Cp/Flu}- ancillaries: {*rac*-Me₂Si(2-Me-Benz[*e*]Ind)₂}ZrCl₂ (**{SBI}-1**), {*rac*-Me₂Si(2-Me-4-Ph-Ind)₂}ZrCl₂ (**{SBI}-2**), {Me₂C(3,6-*t*Bu₂-Flu)(2-Me-4-*t*Bu-Cp)}ZrCl₂ (**{Cp/Flu}-1**), {Ph(H)C(3,6-*t*Bu₂-Flu)(2-Et-4-*t*Bu-Cp)}ZrCl₂ (**{Cp/Flu}-2**), {Ph₂C(2,7-*t*Bu₂-Flu)(2-Me-4-*t*Bu-Cp)}ZrCl₂ (**{Cp/Flu}-3**), {Ph(H)C(2,7-*t*Bu₂-Flu)(2-Me-4-*t*Bu-Cp)}ZrCl₂ (**{Cp/Flu}-4**). The influence of different activation parameters, such as aging time and nature of coactivator (MAO vs boraluminoxane), has been investigated. It was found that the activation efficiency of {Cp/Flu}-type precatalysts by MAO is similar (1–12% at 30 °C) to that of the {SBI}-type precatalysts (4–18%). More, the propagation rates for the {Cp/Flu}-based systems appeared to be superior to those obtained with the {SBI}-type congeners. Deactivation processes, arising from monomer 2,1-misinsertions and resulting in dormant M-*sec*-alkyl species, were demonstrated to occur for both types of catalytic systems. While the {SBI}-type systems are capable to undergo further regular 1,2-insertions of 1-hexene into the M-*sec*-alkyl (or undergo regeneration of an active species through β-H elimination), the {Cp/Flu}-type congeners are apparently reluctant to further enchainment; this is proposed to account for the observed overall lower productivity of the latter {Cp/Flu}-type systems. Dormant M-*sec*-alkyl species with the {Cp/Flu} ancillaries can be efficiently reactivated by introduction of small molecules (H₂ or ethylene).

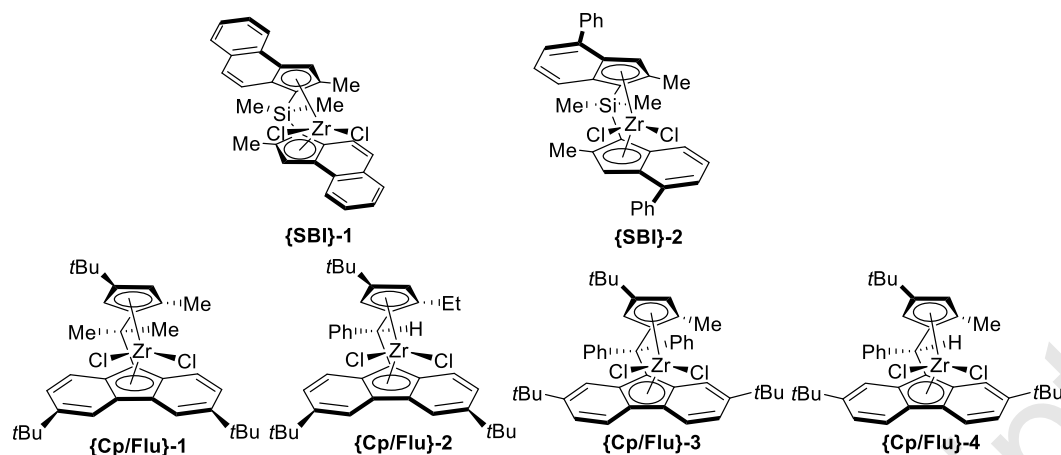
INTRODUCTION

The activity of a catalytic system involved in a complex, multi-step process is mainly determined by the rate of the rate-determining step, that is in most cases $d[\text{substrate}]/dt = -k[\text{substrate}][\text{catalyst}]$, where $[\text{catalyst}]$ is the concentration of catalyst in its active form. Though it is generally accepted for regular catalytic processes a quantitative transformation of catalyst precursor into an active form (*i.e.*, 100% activation efficiency, usually applied for calculation of TON/TOF values), for Ziegler-Natta-type polymerization processes, the typical fraction of active catalyst (χ^*) is often much inferior ($\ll 50\%$ of $[\text{precatalyst}]_0$, depending on the nature of both precatalyst and cocatalyst/coactivator).^{1,2,3,4} In order to get a better understanding of the behavior of a Ziegler-Natta-type catalyst system (precatalyst + coactivator), a comprehensive kinetic analysis is required to determine the activation efficiency as well as the rate constants relative to each step of the polymerization process: initiation, polymer chain growth (propagation) and termination. Besides, insight on possible deactivation processes resulting in decay of active sites is another mandatory information, which could be reasonably used for engineering more efficient catalytic systems reluctant towards side reactions.

In their pioneering work, Fink *et al.*⁵ have reported on the elucidation of primary mechanistic steps of ethylene polymerization by $\text{Cp}_2\text{TiRCl}/\text{AlR}_2\text{Cl}$ ($\text{R} = \text{Me}, \text{Et}$) using stop-flow or quenched-flow (QF) kinetic and ^{13}C NMR labeling techniques. QF techniques have been extended by Terano *et al.*⁶ and Soga *et al.*⁷ to heterogeneous MgCl_2 -supported catalytic systems. Industry-relevant {SBI}- and {EBI}-type group 4-metallocene systems in combination with various cocatalysts (MAO, boranes and borates) have been scrutinized by different QF and labeling methods in polymerization of ethylene, propylene, 1-hexene and 1-octene monomers under homogeneous conditions in prior studies by Busico *et al.*,⁸ Landis *et al.*,^{9,10,11} Bochmann *et al.*¹² and others.^{13,14,15} The estimated activation efficiency reported for

{SBI}-based catalysts ranged from 8 to 25% for polymerization of propylene, and up to 57% for polymerization of 1-hexene. Noteworthy, these values were found to be much dependent on the analytic technique implemented and on the reaction conditions.¹ Among the noted parameters affecting to some extent the concentration of active sites in polymerization of ethylene and α -olefins are polymerization temperature, monomer concentration, nature of cocatalyst and/or scavenger and their concentrations (as determined by the [cocatalyst/scavenger]/[M] ratio).

In this contribution, we aimed at understanding the so-far unknown origin of the much different productivity and possible different behavior between isoselective {SBI}-¹⁶ and {Cp/Flu}-type¹⁷ propylene polymerization precatalysts (Scheme 1); the former catalysts are indeed typically one order of magnitude more productive than the latter systems ($15 \cdot 10^4$ vs $14 \cdot 10^3$ kgPP \cdot mol⁻¹ \cdot h⁻¹, respectively, at 60 °C, 5 bar), both under homogeneous, but also under heterogeneous (supported) conditions. For these studies, a kinetic method developed by Bochmann *et al.*^{12d} was utilized, which is based on determination of the time dependence of monomer conversion and M_n of polymer in polymerization of 1-hexene. This method features the following main advantages: (i) use of a liquid monomer facilitating manipulations, (ii) a relatively slow polymerization kinetic regime, enabling sampling of reaction mixtures aliquots for monitoring, and (iii) polymer products (poly(1-hexenes)) soluble in various solvents, including hydrocarbons, facilitating their analyses. Thus, the catalytic systems composed of zirconocene complexes belonging to both {SBI}- and {Cp/Flu}-families, **{SBI}-2** and **{Cp/Flu}-1-4** (Scheme 1), respectively, and MAO as coactivator were investigated by kinetic QF techniques. Since the methodology and reaction conditions are crucial in order to get relevant and informative data for comparison purposes, the reference system **{SBI}-1/MAO** was also studied and the results were benchmarked with those of Bochmann and coworkers.^{12d}



Scheme 1. Structures of zirconocene precatalysts used in this study.

RESULTS AND DISCUSSION

The same conditions as those originally used for the quenched-flow protocol of Bochmann *et al.*^{12d} were used, that is a mixture of zirconocene complex and MAO was aged over 1 h in toluene at 30 °C prior to the addition of 1-hexene. The apparent propagation rate constant k_p^0 was calculated from the (polymer yield) = $f([Zr]_0)$ and (polymer yield) = $f(\text{time})$ fits, obtained at low conversions ($\leq 20\%$) of monomer, according to equation 1 (see the Experimental section) developed using the approximation of initial rates. The specific propagation and termination rate constants, k_p^B and k_t^B , respectively, were extracted from the M_n (or DP_n) = $f(\text{time})$ data (equation 2) using a curve-fitting procedure. Also, the impact of different conditions on the polymerization kinetics was scrutinized: (a) nature of solvent (*n*-heptane vs toluene), (b) aging time, (c) temperature, and (d) nature of cocatalyst (boraluminoxane vs MAO).

Polymerizations in toluene. The value of k_p^0 determined for the benchmark system {SBI}-1/MAO (Table 1, Fig. S1) under our conditions was found to be in good agreement with those reported by Bochmann and coworkers^{12d} (k_p^0 , 0.30(3) vs 0.17(1)–0.47(5) L·mol⁻¹·s⁻¹). On the other hand, the value of k_p determined from a non-linear regression of

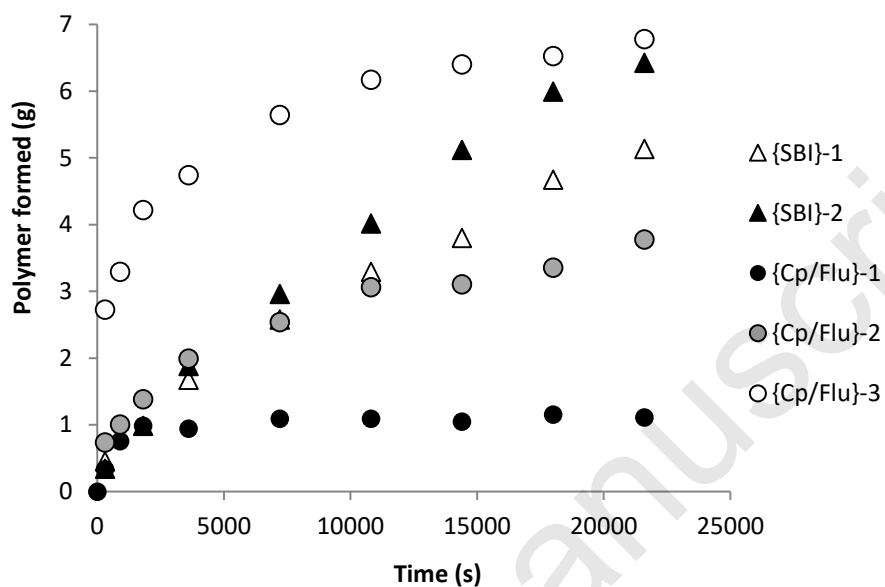
equation (2) for the $DP_n = f(\text{time})$ data, repeatedly obtained at < 20% conversion of monomer, was of 7(2) $\text{L}\cdot\text{mol}^{-1}\cdot\text{s}^{-1}$, which is significantly larger than the reported values of 1.02(2)–1.28(5) $\text{L}\cdot\text{mol}^{-1}\cdot\text{s}^{-1}$.^{12d} In order to elucidate the origin of this discrepancy, the experimental $DP_n = f(\text{time})$ data from ref.^{12d} were reprocessed (Fig. S2). Using exclusively the data points obtained in each case at early stages of polymerization (i.e., monomer conversion < 20%), the non-linear regression procedure returned a set of values of k_p^B and k_t^B (4(1)–9(4) $\text{L}\cdot\text{mol}^{-1}\cdot\text{s}^{-1}$ and $1.2(4)$ – $3(2)\cdot 10^{-2} \text{ s}^{-1}$, respectively), different from those reported in the original paper but very close to those obtained in the present study (Table 1, entry 1). In parallel, the reported values of rate constants were used to plot the corresponding kinetic curves. The resulting plots exhibited a substantial deviation from the experimental data points at early polymerization stages and followed the experimental trend only at large monomer conversions ($\gg 20\%$). These observations indicate that in ref.^{12d} the data obtained at latter polymerization stages were used for calculation of the corresponding rate constants. For better consistency and to allow meaningful comparisons, we have used in the present study only values determined at low monomer conversions, i.e. at early polymerization stages.

Alternatively, the propagation and termination rate constants k_p^N and k_t^N were evaluated using Natta's equation (3), thus affording a complementary set of data. Depending on the value of k_p , the fraction of active sites χ^* for system **{SBI}-1/MAO** varied from 4(2) to 8(2)%, but this remains within the accuracy of the methods. For the sake of conformity, in the following, the values of k_p^B and χ^* calculated from equation (2) will be systematically used for comparison.

For **{SBI}-2**, the kinetic plot of polymer yield vs time (Fig. 1) is similar to that obtained with **{SBI}-1/MAO**, especially at early polymerization stages. The value of k_p^0 determined for this system (Fig. S3) is nearly twice of that observed for **{SBI}-1/MAO** (Table 1, entries 2 and 1). At the same time, the propagation rate constant k_p is twofold smaller,

which makes the fraction of active species, determined from the ratio k_p^0/k_p , to be significantly higher for {SBI}-2 as compared to that found for the reference precatalyst {SBI}-1 (0.18(8) vs 0.04(2), respectively).

a)



b)

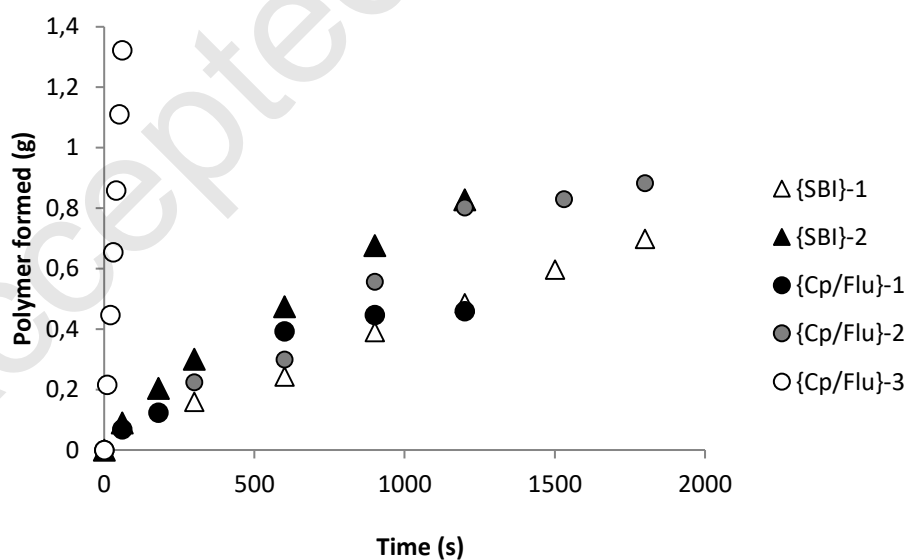


Figure 1. Overview of kinetic experiments with different precatalysts: aging time = 60 min; $T_{\text{aging}} = T_{\text{polym}} = 30\text{ }^{\circ}\text{C}$; $[\text{Zr}]_{\text{tot}} = 0.20\text{ mM}$; $[\text{1-hexene}]_0 = 1.6\text{ M}$ in toluene (6.73 g, 80.5 mmol);

[MAO]/[Zr]_{tot} = 1000; a) kinetic data obtained over 6 h, resulting in high depletion of monomer (conversions close to 100 % for **{SBI}-2** and **{Cp/Flu}-3**); b) kinetic data obtained at ≤ 20% monomer conversion and used for calculation of the apparent propagation rate constant k_p^0 .

Interestingly, for **{Cp/Flu}-1** and **{Cp/Flu}-2** (Fig. S4 and S5, respectively), the apparent propagation rate constants ($k_p^0 = 0.52(6)$ and $0.47(5)$ L·mol⁻¹·s⁻¹, respectively) calculated at the early stages of polymerization are comparable or very close to those obtained for the **{SBI}**-based counterparts; however, the specific propagation rate constants ($k_p = 8.2(7)$ and $52(8)$ L·mol⁻¹·s⁻¹, respectively) were found to be one order of magnitude higher, which returned quite poor activation efficiency for both systems ($k_p^0/k_p = 0.06(2)$ and $0.009(2)$, respectively). Yet, the overall activities of these systems rapidly decreased over time: no further monomer conversion was observed after several hours (ca. 0.5 and 8 h, respectively). This obviously reflects deactivation of active species (vide infra). Gratifyingly, the **{Cp/Flu}-3/MAO** system followed perfect first-order kinetics under these conditions, leading to full conversion of 1-hexene after 6 h, and yielded the highest k_p^0 and k_p values within the whole series (Fig. S6; $16(5)$ and $131(42)$ L·mol⁻¹·s⁻¹, respectively). Nearly the same kinetic profile (Fig. S7) as for the **{Cp/Flu}-3/MAO** system was obtained for the close analogue **{Cp/Flu}-4/MAO** having different substituents on the ligand bridge (Ph₂C vs Ph(H)C, respectively), thus emphasizing the minor impact of this parameter on catalytic activity.

The poly(1-hexene) samples obtained with **{SBI}-2** and **{Cp/Flu}-1-3** were analyzed by ¹H NMR spectroscopy (Fig. S23), and the nature of the unsaturated chain-end groups was identified. For all samples, the corresponding regions of the spectra showed only two types of signals: two singlets assigned to the two hydrogens of vinylidene end-groups (δ 4.76 and 4.70

ppm) and multiplet (δ 5.35–5.45 ppm) for internal $-CH=CH-$ moieties. While the former groups arose from a regular chain termination reaction, i.e. β -H elimination after primary (1,2-) insertion of monomer, the possible origin of the latter multiplet is β -H elimination after secondary (2,1-) insertion of monomer.¹⁸ Noteworthy, for poly(1-hexene)s obtained with **{SBI}-2/MAO**, the relative abundance of the internal $-CH=CH-$ groups is significantly higher than that of vinylidene end-groups; this suggests that the chain release process via β -H elimination after 2,1- insertion predominates for this system.

Table 1. Values of k_p^0 , k_p (in $L \cdot mol^{-1} \cdot s^{-1}$) and k_t (in $10^{-2} \cdot s^{-1}$) for different zirconocene/MAO systems.

Entry	Catalyst	k_p^0 ^a	k_p ^{B b,c}	$k_t^B (10^{-2})$ ^{b,c}	k_p^0/k_p^B	k_p^N ^d	$k_t^N (10^{-2})$ ^d	k_p^0/k_p^N
1	{SBI}-1	0.30(3) [0.17–0.47] ^{12d}	7(2) [1.02–1.28] ^{12d}	1.8(5) [0.19–0.59] ^{12d}	0.04(2)	4.0(7)	0.9(2)	0.08(2)
2	{SBI}-2	0.53(5)	3(1)	0.9(4)	0.18(8)	2.00(3)	0.5(1)	0.27(3)
3	{Cp/Flu}-1	0.52(9)	8.2(7)	2.5(3)	0.06(2)	5(2)	1.36(8)	0.10(6)
4	{Cp/Flu}-2	0.47(5)	52(8)	7(1)	0.009(2)	35(2)	4.9(3)	0.013(2)
5	{Cp/Flu}-3	16(5)	131(42)	13(5)	0.12(6)	76.1(1)	7(1)	0.21(1)

See Figure 1 for reaction conditions, unless otherwise stated. ^a Determined with equation (1). ^b Determined with equation (2) from the $M_n = f(\text{time})$ data. ^c The value of k_i was fixed at $3.8 L \cdot mol^{-1} \cdot s^{-1}$. ^d Determined with equation (3).

Influence of aging conditions. The influence of aging conditions was investigated for **{SBI}-2** (Fig. S8), **{Cp/Flu}-1** (Fig. S9), **{Cp/Flu}-2** (Fig. S10) and **{Cp/Flu}-3** (Fig. S11). The reactions were conducted with different aging durations, temperatures (30 °C or 60 °C), and in the presence of 1-hexene (pre-polymerization). Representative data are summarized in Table 2.

For the **{SBI}-2/MAO** system, no significant influence of the aging conditions on activity was observed; the propagation rate constants k_p^0 calculated at 2 and 60 min of aging were very close (entries 2 and 1, respectively). Also, the amount of active sites as well as molecular weight characteristics remained constant throughout this time period.

For the **{Cp/Flu}-1/MAO** system, complete loss of activity was observed after about 0.5–1 h of polymerization at 30 °C, indicating that the catalyst is totally deactivated after this period. When both aging and polymerization were performed at 60 °C, 1-hexene was fully consumed; however, the yield of polymer recovered (0.80 g) was not consistent with the conversion of 1-hexene observed (Fig. S9) and concomitant formation of 2-hexene from 1-hexene in a side isomerization reaction was evidenced by ¹H NMR spectroscopy. This side reaction also occurred at 30 °C but to a lesser extent (ca. 10% of 2-hexene formed after 6 h). For **{Cp/Flu}-2**, the same isomerization reaction took place at 60 °C giving only 10% of 2-hexene after 6 h, while no isomerization was observed for **{Cp/Flu}-3**. Upon decreasing the aging time from 60 to 10 and 2 min, a significant decrease of activity (as reflected by the k_p values) was observed for the three {Cp/Flu} catalysts (entries 4/5, 7/8 and 10/11, respectively); the trend was more pronounced for the **{Cp/Flu}-1/MAO** system. For the three systems, the fraction of active sites determined at shorter aging time was found systematically higher, thus suggesting degradation of active sites to a significant extent (especially for **{Cp/Flu}-1**) over time during the aging period in the absence of monomer.

Table 2. Values of k_p^0 and k_p (in $\text{L}\cdot\text{mol}^{-1}\cdot\text{s}^{-1}$) determined for {SBI}-1-2/ and {Cp/Flu}-1-3/MAO systems under different conditions.

Entry	Precatalyst	Aging time [min]	k_p^0	k_p^B	k_p^0/k_p^B	M_n [kDa]	D_m
1	{SBI}-2	60	0.30(3)	7(2)	0.33(4)	43.6/44.9 ^{a,b}	1.65/1.61
2	{SBI}-2	2	0.49(5)	4(2)	0.37(7)	50.7 ^{a,c}	1.60
3	{Cp/Flu}-1	60	0.52(9)	8.2(7)	0.06(2)	37.9 ^d	1.25
4	{Cp/Flu}-1	10	0.30(7)	8(1)	0.04(1)	41.9 ^d	1.16
5	{Cp/Flu}-1	2	1.3(2)	2.4(4)	0.5(2)	32.1/30.3 ^d	1.19/1.20
6	{Cp/Flu}-2	60	0.47(5)	52(8)	0.009(2)	87.0/89.1 ^e	1.30/1.33
7	{Cp/Flu}-2	10	1.6(8)	27(4)	0.06(4)	87.1/88.8 ^{a,d}	1.29/1.32
8	{Cp/Flu}-2	2	1.4(3)	12(2)	0.12(2)	76.7/75.2 ^{a,d}	1.29/1.42
9	{Cp/Flu}-3	60	16(5)	131(42)	0.12(6)	115.5 ^f	1.43
10	{Cp/Flu}-3	10	10(5)	220(70)	0.05(2)	109.1/110.2 ^{a,f}	1.45/1.45
11	{Cp/Flu}-3	2	8.8(7)	61(8)	0.14(4)	114.3/115.0 ^{a,d}	1.33/1.34

See Figure 1 for reaction conditions, unless otherwise stated. ^a Results from duplicated experiments. ^b Determined after 20 min of reaction. ^c Determined after 25 min of reaction. ^d Determined after 5 min of reaction. ^e Determined after 3 min of reaction. ^f Determined after 1 min of reaction.

Influence of cocatalyst. Binary boraluminoxane (BMAO) coactivators derived from the reaction between trisalkylaluminum R_3Al and boronic acid $(C_6F_5)B(OH)_2$ have been previously demonstrated as alternative activators to classical MAO, however, requiring bis(alkyl) zirconocene precursors.¹⁹ In particular, the $AlMe_3/(C_6F_5)B(OH)_2$ system used for activation of $\{Me_2Si(Flu)(NtBu)\}TiMe_2$ resulted in a more productive catalyst than that generated from MAO under the same conditions.²⁰ These findings prompted us to probe under similar conditions boraluminoxane activating systems obtained by reaction of trisalkylaluminum R_3Al ($R = Me, iBu$) and $(C_6F_5)B(OH)_2$ in different ratios. Hence, the dimethyl zirconocenes **{SBI}-2a**, **{Cp/Flu}-1a** and **{Cp/Flu}-3a** were used in combination with $AlMe_3/(C_6F_5)B(OH)_2$ or $iBu_3Al/(C_6F_5)B(OH)_2$ under regular¹⁹ polymerization conditions (Fig. S12–S14, Table 3). As a general trend, the boraluminoxanes appeared to be less efficient regardless the nature of precatalyst, as both {SBI}- and {Cp/Flu}-based catalyst systems were one order less active (in terms of k_p^0) as compared to polymerization tests using MAO. The $AlMe_3$ -based coactivator was less efficient for both types of zirconocene families (entries 2 and 9), while for $iBu_3Al/(C_6F_5)B(OH)_2$ an optimal ratio of 100:50 was found so far to exhibit a better performance within the whole series of experiments using BMAOs as coactivators (entries 4 and 11). Importantly in the frame of this study, in line with the results obtained with MAO, the systems based on **{Cp/Flu}-1a** appeared to be less active within the whole series of precursors. Also, for the both BMAO-activated {Cp/Flu}-type systems, the corresponding kinetic plots (Fig. S13 and S14, respectively) exhibited a marked decrease of activity after ca. 2 h of reaction, comparable to that observed with MAO-based systems. Overall, these observations suggest that the deactivation processes are independent of the nature of the coactivator.

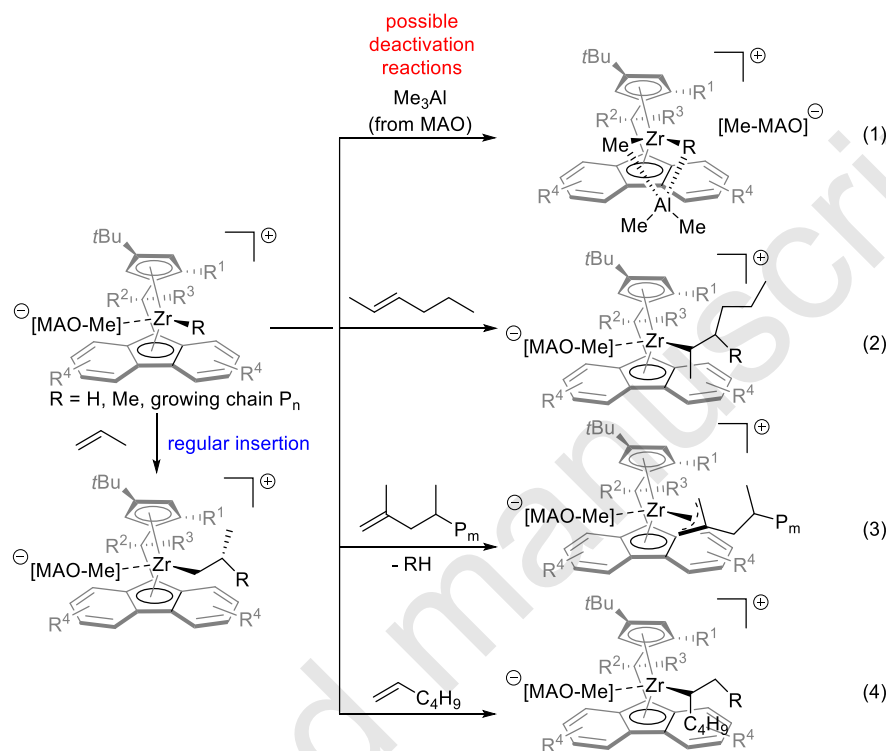
Table 3. Values of k_p^0 (in $L \cdot mol^{-1} \cdot s^{-1}$) determined for **{SBI}-2a**, **{Cp/Flu}-1a** and **{Cp/Flu}-3a** using boraluminoxane coactivators.^a

Entry	Precatalyst	Coactivator (equiv vs Zr)	k_p^0	M_n [kDa]	D_m
1	{SBI}-2	MAO (1000)	0.53(5)	74.4	1.63
2	{SBI}-2a	AlMe ₃ (100)/ ArB(OH) ₂ (100)	0.08(5)	31.2	1.51
3	{SBI}-2a	TIBAL (100)/ ArB(OH) ₂ (100)	0.05(2)	53.9	1.46
4	{SBI}-2a	TIBAL (100)/ ArB(OH) ₂ (50)	0.19(5)	73.6	1.40
5	{Cp/Flu}-1	MAO (1000)	0.52(9)	71.7	1.42
6	{Cp/Flu}-1a	TIBAL (100)/ ArB(OH) ₂ (50)	0.07(3)	149.0	1.41
7	{Cp/Flu}-1a	TIBAL (100)/ ArB(OH) ₂ (50) ^b	0.1(1)	168.2	1.64
8	{Cp/Flu}-3	MAO (1000)	16(5)	92.3	1.66
9	{Cp/Flu}-3a	AlMe ₃ (100)/ ArB(OH) ₂ (100)	0.20(7)	161.8	1.34
10	{Cp/Flu}-3a	TIBAL (100)/ ArB(OH) ₂ (100)	1.0(3)	225.4	1.46
11	{Cp/Flu}-3a	TIBAL (100)/ ArB(OH) ₂ (50)	2(2)	169.4	1.42
12	{Cp/Flu}-3a	TIBAL (100)/ ArB(OH) ₂ (20)	0.08(3)	132.0	1.66

^a General polymerization conditions, unless otherwise stated: a mixture of (C₆F₅)B(OH)₂ and R₃Al was stirred overnight at 60 °C; aging time = 2 min, $T_{aging} = T_{polym} = 30$ °C. ^b DIBAL-H (100 equiv.) was added during aging.

Studies on the deactivation and reactivation of {Cp/Flu} systems. The decreasing activity of systems based on **{Cp/Flu}-1,2** over time at 30 °C and the deactivation observed with **{Cp/Flu}-3** at higher polymerization temperature may have similar origins. Four main hypotheses may be considered to account for those phenomena (Scheme 2): (1) active cationic species slowly and irreversibly binds AlMe₃ contained in/generated from MAO to afford robust inactive AlMe₃-adducts;^{3a} (2) 2-hexene, concomitantly produced as an isomerization side-product (*vide supra*), reinserts into M–C (or M–H) bonds, yielding “inactive” *sec*-alkyl species; (3) formation of inactive allylic species via alkane elimination reactions between

alkyl-zirconocene active species and vinylidene end-capped polymer chains, produced by regular β -H elimination reactions;^{10e,14,21,22} (4) formation of “inactive” *sec*-alkyl species (alike those formed in (2)) via 2,1-misinsertion of 1-hexene into the M–C (or M–H) bond of a propagating species.²³



Scheme 2. Main putative deactivation pathways affording stable products for polymerization catalyzed by {Cp/Flu}-based zirconocene complexes.

To probe the two first deactivation pathways, (1) and (2), a kinetic monitoring was performed for polymerizations conducted with **{Cp/Flu}-1** in the presence of AlMe_3 -depleted MMAO (i.e., MAO modified by 2,6-di-*tert*-butyl-4-methylphenol, BHT)²⁴ or of 2- or 3-hexene (Fig. S15 and S16, respectively). In both cases, very similar kinetic profiles (in terms of monomer conversion as a function of time) to those obtained for the original polymerization reactions were observed; this suggests that neither excess AlMe_3 nor internal olefins interfere in the deactivation process of this catalytic system under such conditions.

This is consistent with the observation that deactivation takes place also in the presence of boraluminoxanes (*vide supra*). These results provide an alternative rationale to our previous hypothesis,²⁵ which suggested the possible crucial role of AlMe₃ in catalyst deactivation via the formation of stable heterobimetallic AlMe₃-zirconocene adducts.

Formation of stable allyl-zirconocenes has been reported to contribute up to 90% of the total metallocene catalyst concentration.^{10e,14,21,22} Alternatively, 2,1-misinsertion of the monomer into the M–C bond of the growing polymeric chain (4)²³ has been proposed as a competitive, and sometimes predominant, reaction towards formation of “dormant” states.^{13,10a,12} The “dormant” states generated in the two above deactivation processes, albeit much less prone to insert α -olefins, are not completely unreactive and can be back converted to propagating species by reactions with smaller molecules. For instance, Cipullo *et al.*²⁶ recently reported on the deactivation of propylene polymerization with MgCl₂-supported Ziegler-Natta catalysts via 2,1-misinsertions and reactivation of the dormant state by a deliberate introduction of dihydrogen, which is generally used as a chain-transfer agent (CTA). Prompted by the above results, we investigated how 1-hexene polymerization catalyzed by the {Cp/Flu}-type zirconocene complexes could be reactivated by introduction of hydrosilanes (Ph₂SiH₂ and PhSiH₃) or dihydrogen as CTA, and also of ethylene, a smaller, much more reactive monomer.

A two-shot introduction of Ph₂SiH₂ and PhSiH₃ (20 and 50 equiv. with respect to [Zr]₀) in a polymerization reaction carried out under regular conditions with the {**Cp/Flu**}-1/MAO system did not change the overall kinetic profile (Fig. S17) as compared to that observed in the absence of hydrosilanes. At this point, we surmise that hydrosilanes are either nonreactive or consumed instantly in a chain-transfer reaction and therefore cannot influence either the general profile of the propagation or the overall activity of the system.

Alternatively, dihydrogen (80 mL at 1 bar pressure, ca. 7 mg ($[\text{H}_2]_0/[\text{Zr}]_{\text{tot}} = 350$)) was introduced in the polymerization reaction in one shot at a time when the system **{Cp/Flu}-1/MAO** was no longer active (after 10,000 sec of reaction; Fig. 2). A nearly immediate burst in monomer conversion was noted. Yet, the amount of polymer recovered in this experiment after 14,400 sec (2.23 g, 33%) did not match the overall observed conversion of 1-hexene (80%) and isomerization of 1-hexene to 2-hexene (about 35%) was evidenced from the ^1H NMR spectra of the reaction mixture.²⁷ Hence, the presence of dihydrogen with **{Cp/Flu}-1/MAO** eventually regenerated active species (i.e., zirconocene-hydrido) but the latter also favored side isomerization (and transfer/hydrogenation) reactions.

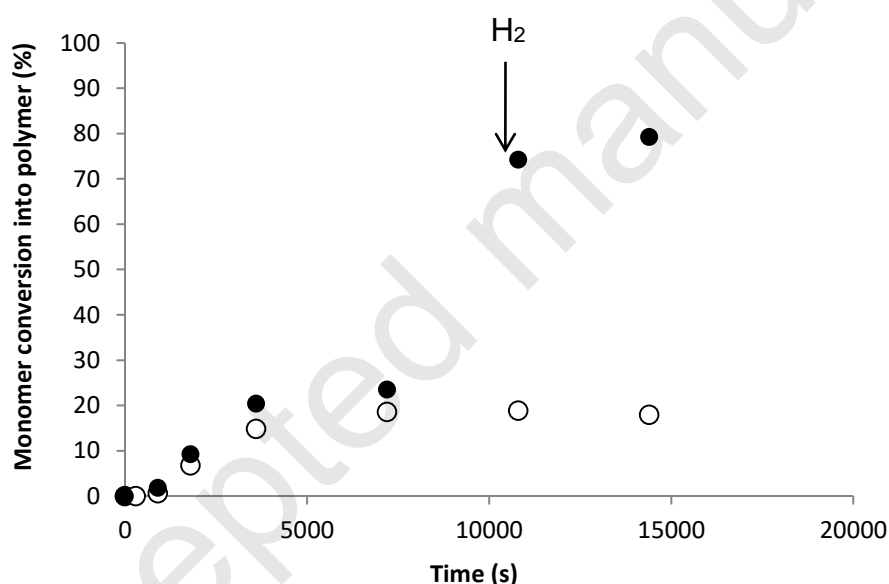


Figure 2. Kinetic plots of 1-hexene polymerizations performed with **{Cp/Flu}-1/MAO** in the absence (○) or after introduction of dihydrogen after 120 min (●). Conditions: Aging time = 2 min, $T_{\text{aging}} = T_{\text{polym}} = 30\text{ }^\circ\text{C}$, $[\text{Zr}]_{\text{tot}} = 0.20\text{ mM}$, $[\text{MAO}]/[\text{Zr}]_{\text{tot}} = 1000$, $[\text{1-hexene}]_0/[\text{Zr}]_{\text{tot}} = 8060$, toluene.

More informatively, a one-shot addition of a small amount of ethylene (80 mL at 1 bar pressure, ca. 0.1 g,) to the “dormant” polymerization reaction with **{Cp/Flu}-1/MAO** after a period of 7200 sec resulted in restoration of activity of the system (Fig. 3). In a separate

experiment, similar small amounts of ethylene were introduced three times into the same polymerization reaction, which allowed eventually achieving 65% conversion of monomer (Fig. 3). Noteworthy, the THF-soluble poly(1-hexene)-*co*-ethylene copolymers obtained in the two last experiments featured monomodal and quite narrow ($D_m = 1.46$) molecular weight distributions (Table 4), very close to that obtained in 1-hexene homopolymerization in the absence of ethylene. These results unequivocally evidence uniform incorporation of ethylene into growing polymer chains as well as efficient transformation of the “dormant” state of catalyst into the propagating state.

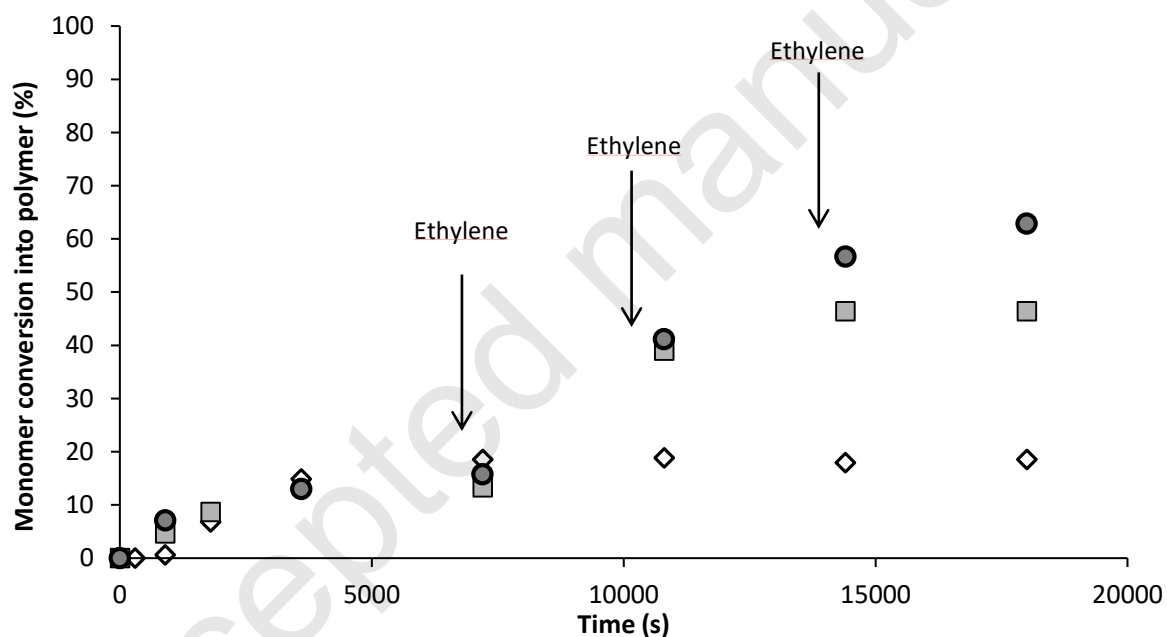


Figure 3. Kinetic plots of 1-hexene polymerizations performed with $\{\text{Cp}/\text{Flu}\}\text{-1}/\text{MAO}$ in the absence (\diamond) or after introduction of ethylene once (80 mL at 1 bar, ca. 0.1 g) (\blacksquare) or three times ($3 \times$ ca. 0.1 g) (\bullet). Conditions: Aging time = 2 min, $T_{\text{aging}} = T_{\text{polym}} = 30$ °C, $[\text{Zr}]_{\text{tot}} = 0.20$ mM, $[\text{MAO}]/[\text{Zr}]_{\text{tot}} = 1000$, $[\text{1-hexene}]_0/[\text{Zr}]_{\text{tot}} = 8060$, toluene.

Table 4. Effect of ethylene addition on 1-hexene polymerization catalyzed by **{Cp/Flu}-1/MAO** (data from kinetic plots depicted on Fig. 3).

Entry	Ethylene addition [g]	Mass of polymer isolated [g]	M_n [kDa]	D_m
1	-	0.8	72.5	1.32
2	1×0.1	3.4	83.1	1.47
3	3×0.1	4.4	77.7	1.46

In order to get a better insight into the nature of “dormant” forms of **{Cp/Flu}**-based olefin polymerization catalysts, which are apparently reactivated by addition of ethylene, the microstructures of the corresponding poly(olefin)-*co*-ethylene copolymers can be scrutinized by ^{13}C NMR spectroscopy.²⁸ In our case, analysis of the obtained poly(1-hexene)-*co*-ethylene copolymers turned not to be possible due to overlapping of the ^{13}C NMR signals from the methylenic groups resulting from the small amount of incorporated ethylene and those from polyhexene. Therefore, the corresponding poly(propylene-*co*-ethylene) copolymers both incorporating ca. 3 mol% of ethylene ($M_n = 48.3$ and 86.5 kDa; $M_w/M_n = 3.11$ and 2.30, respectively) were prepared using **{SBI}-2/MAO** (for comparison) and **{Cp/Flu}-1/MAO** catalytic systems and analyzed by $^{13}\text{C}\{^1\text{H}\}$ NMR spectroscopy (Fig. 4). For **{SBI}-2**, the signals at δ 42.3, 38.6, 36.0, 31.5, 30.6, 29.4, 17.6 and 17.2 ppm, assigned to the isolated 2,1-misinsertions equally distributed in the “pure” polypropylene segments,²⁸ were quantified at 0.36%. The resonances at δ 34.8, 34.6, 34.0 and 31.3 ppm arising from ethylenic units situated right after 2,1-regioerrors²⁹ were quantified at 0.33%. Thus, the total content of 2,1-regioerrors of 0.7% is close to that (0.3%) reported for ethylene-propylene copolymers obtained with the same catalyst by Busico *et al.*²⁸ For **{Cp/Flu}-1**, only traces (0.02%) of 2,1-insertions were found in the copolymer and, apparently (as far as the detection limit and signal-to-noise ratio allow), those were systematically followed by ethylene units (Fig. 4, bottom); no signals were observed that would correspond to isolated 2,1-regioerrors in “pure”

polypropylene sequences (i.e., without being enchainned to a subsequent ethylene unit). These observations are in agreement with the intrinsic competence of the {SBI}-based systems to propagate, even in a chain resulting from a 2,1-misinsertion (either by further insertion or regeneration of an active hydrido species through β -H elimination; vide supra). On the other hand, for the {Cp/Flu}-based systems, even though 2,1-misinsertions are far less frequent than for the former {SBI}- systems, they apparently result in species strongly reluctant to insertion reactions of monomer bulkier than ethylene (α -olefins).

It should be noted that no signals from internal vinylidene unsaturations,^{9e,30,31} which would have resulted from allylic activation (Scheme 2, pathway (3)), were found in the spectra of the poly(propylene-*co*-ethylene) copolymers. This suggests that this particular deactivation pathway is not feasible with both catalytic systems (at least, under the given conditions).

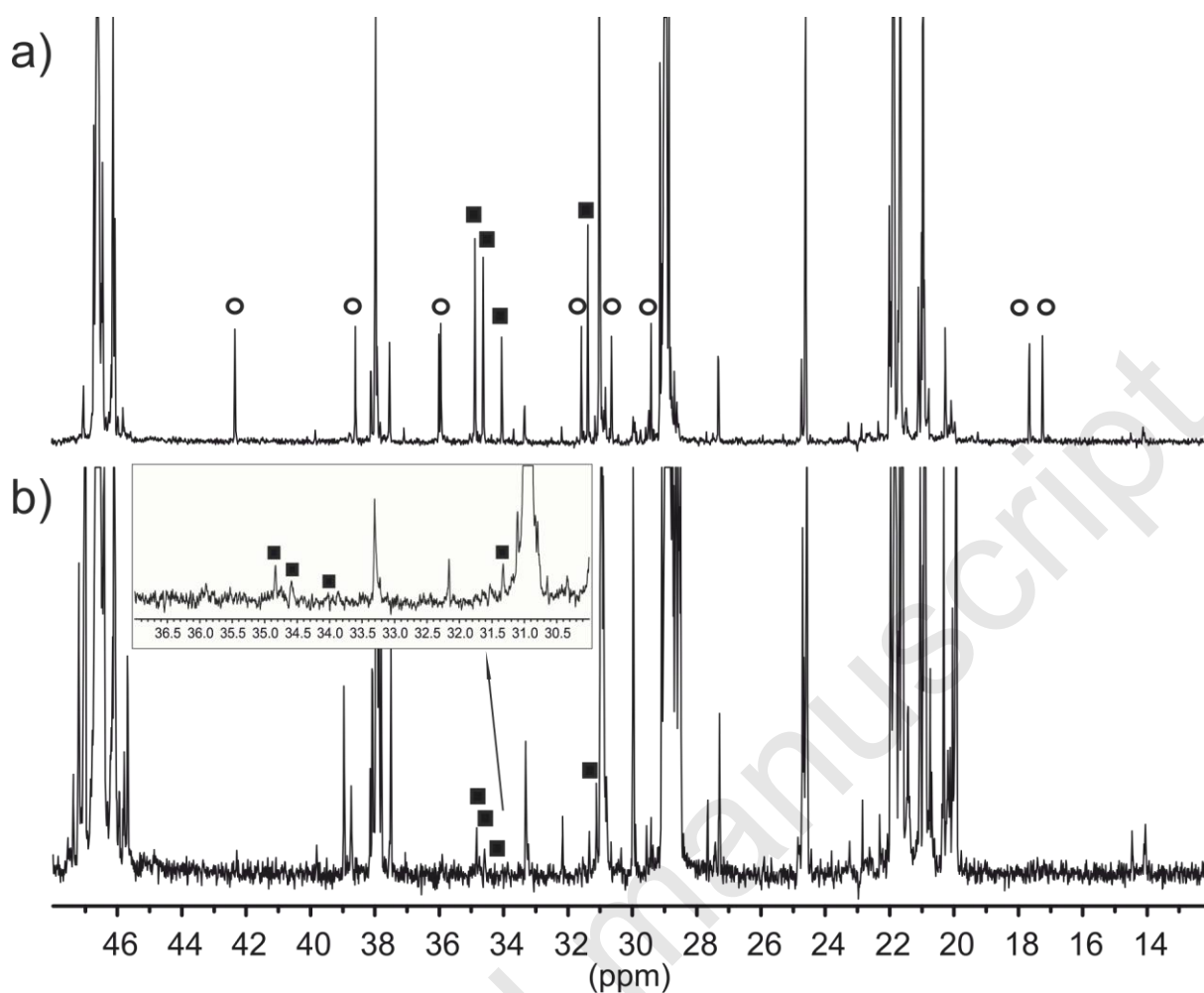


Figure 4. Details of the $^{13}\text{C}\{^1\text{H}\}$ NMR spectra (125 MHz, 135 °C, 1,2,4-trichlorobenzene/ C_6D_6 4:1 v/v) of poly(propylene-co-ethylene) copolymers obtained with a) {SBI}-2/MAO and b) {Cp/Flu}-1/MAO systems: ○ – 2,1-propylene misinsertions, ■ – ethylenic units after 2,1-misinsertions.

Conclusions

In this contribution, kinetic investigations were conducted in order to evaluate the efficiency of two important propylene polymerization catalytic systems, namely {SBI}- and {Cp/Flu}-type zirconocene complexes, via determination of the propagation rate constants k_p^0 and k_p and the fraction of active species generated. The kinetic data obtained indicated a slightly inferior activation efficiency for {Cp/Flu}-type precatalysts (1–12%) as for the overall more productive {SBI}-type precatalysts (4–18%) under identical conditions.

Noteworthy, the propagation rate constants k_p for 1-hexene polymerization reactions catalyzed by {Cp/Flu}-based systems are at least one order larger than those for the {SBI}-type catalysts. However, the {Cp/Flu}-based systems generate by 2,1-misinsertion of α -olefin M-*sec*-alkyl species that appear much reluctant to further propagation. The corresponding species formed by 2,1-misinsertion in the case of the {SBI}-based systems, although much more frequent than for the {Cp/Flu}-based systems (0.36 vs 0.02 mol%, respectively), are still reactive and can either further propagate or regenerate an active hydrido species upon β -H elimination. Among the factors enabling efficient reactivation of the {Cp/Flu}-based systems is introduction of such small molecules as ethylene and dihydrogen in the polymerization reaction. Hence, rather ironically, the {Cp/Flu}-based systems are intrinsically more active and less prone to 2,1-misinsertions than the {SBI}-systems, but the very few resulting regiodefects seem to be much more deleterious than their {SBI}-analogues. Though the above kinetic results were obtained for polymerization of 1-hexene, we assume that the conclusions can be most likely transposed to propylene polymerization.

In our previous study,²⁵ using the obtained spectroscopic data for these two families of isoselective zirconocene catalytic systems, we have highlighted the formation of heterobimetallic AlMe₃-zirconocene adducts; those species derived from {Cp/Flu} complexes proved much more stable than their {SBI}-analogues. On this basis, we initially hypothesized the plausible deleterious role of AlMe₃ as the main origin for the lower productivity of {Cp/Flu}-type catalysts.²⁵ The present kinetic study provides a clear but quite different rationale. Understanding the role of different structural elements and factors (steric and electronic) responsible for such discrepancy in polymerization behaviors of these two zirconocene systems will allow engineering of new {Cp/Flu}-type catalysts, more efficient in terms of activity, productivity, number of active sites and resistance to side reactions. These investigations are underway in our labs.

EXPERIMENTAL SECTION

Materials. All manipulations were performed under a purified argon atmosphere using standard Schlenk techniques or in a glovebox. Solvents were distilled from Na/benzophenone (THF, Et₂O) and Na/K alloy (toluene, pentane) under nitrogen, degassed thoroughly and stored under nitrogen prior to use. Deuterated solvents (benzene-*d*₆, toluene-*d*₈, THF-*d*₈; >99.5% D, Deutero GmbH and Euroisotop) were vacuum-transferred from Na/K alloy into storage tubes. CDCl₃, CD₂Cl₂ and C₂D₂Cl₄ were kept over CaH₂ and vacuum-transferred before use. MAO (30 wt-% solution in toluene, Albermale; contains ca. 10 wt-% of free AlMe₃) was used as received. 1-Hexene (Acros) was distilled from CaH₂ under argon and kept over molecular sieves 3A. Propylene (99.9%, Air Liquide) was used without further purification. The precursors {Me₂C(3,6-*t*Bu₂-Flu)(2-Me-4-*t*Bu-Cp)}ZrCl₂ (**{Cp/Flu}-1**)³² and {Ph(H)C(3,6-*t*Bu₂-Flu)(2-Et-4-*t*Bu-Cp)}ZrCl₂ (**{Cp/Flu}-2**)^{17c} were synthesized as described in the patent literature, while **{Cp/Flu}-3** was provided by Total-Raffinage Chimie. Dimethyl zirconocenes **{SBI}-2a** and **{Cp/Flu}-1a** were prepared from the corresponding dichloro precursors using published procedures²⁵ and characterized by ¹H NMR spectroscopy and elemental analysis prior to use. Other starting materials were purchased from Alfa, Strem, Acros and Aldrich, and used as received.

Instruments and Measurements. ¹³C{¹H} NMR analyses of polypropylene homo- and PP-*co*-PE copolymer samples were performed in the research center of Total Raffinage Chimie in Feluy (Belgium) on a AM-500 Bruker spectrometer equipped with a cryoprobe using the following conditions: solutions of ca. 200 mg of polymer in trichlorobenzene/C₆D₆ (2:0.5 v/v) mixture at 135 °C in 10 mm tubes, inverse gated experiment, pulse angle = 90°, delay = 11 s, acquisition time = 1.25 s, number of scans = 6,000.

Size exclusion chromatography (SEC) analyses of poly(1-hexene) samples were performed in THF (1.0 mL·min⁻¹) at 20 °C using a Polymer Laboratories PL-GPC 50 plus 25(PL-LS 45/90) detectors. The number-average molecular masses (M_n) and polydispersity index (D_m) of the polymers were calculated with reference to a universal calibration vs polystyrene standards.

Synthesis of {Ph₂C(2,7-*t*Bu₂Flu)(3-*t*Bu-5-MeCp)}ZrMe₂ ({Cp/Flu}-3a). To a solution of {Cp/Flu}-3 (1.00 g, 1.35 mmol) in toluene (30 mL) was added MeMgBr (1.00 mL of a 3.0 M solution in Et₂O, 2.97 mmol) at -30 °C under stirring. The resulting solution was allowed to warm up to room temperature and stirred at 60 °C for 2 h. Then volatiles were evaporated in vacuo and hexane (ca. 50 mL) was vacuum transferred in under reduced pressure. The mixture was filtered and the solvent was removed from filtrate to give an orange powder, which was dried under vacuum to give {Cp/Flu}-3a (0.82 g, 1.17 mmol, 87%). ¹H NMR (C₆D₆, 400 MHz, 25 °C): δ 8.10 (m, 1H, ArH), 8.03 (m, 2H, ArH), 7.80 (m, 1H, ArH), 7.64 (m, 2H, ArH), 7.47 (m, 2H, ArH), 7.18 (m, 2H, ArH), 7.05 (m, 3H, ArH), 6.90 (m, 2H, ArH), 6.36 (m, 1H, Flu), 6.20 (d, ⁴J = 3.0, 1H, Cp), 5.67 (d, ⁴J = 3.0, 1H, Cp), 1.86 (s, 3H, CH₃), 1.22 (s, 9H, CCH₃-Flu), 1.17 (s, 9H, CCH₃-Flu), 1.11 (s, 9H, CCH₃-Cp), -0.96 (br s, 6H, ZrCH₃). ¹³C{¹H} NMR (C₆D₆, 100 MHz, 25 °C) (some signals from quaternary carbons overlapped with those from solvent): δ 149.0, 148.2, 147.8, 145.3, 137.7, 130.4, 129.7, 129.6, 128.8, 126.6, 126.5, 126.3, 125.5, 123.7, 123.5, 123.4, 121.4, 121.3, 120.2, 119.6, 118.0, 114.7, 102.3, 100.3, 75.8, 59.9, 37.2, 35.4 (ZrCH₃), 35.1 (ZrCH₃), 34.4, 33.0, 31.3 (CCH₃), 31.1 (CCH₃), 30.7 (CCH₃), 19.9 (CCH₃). Anal. Calcd for C₄₆H₅₄Zr: C, 79.14; H, 7.80. Found: C, 79.04; H, 7.86.

Kinetic investigations. To estimate the amount of active species generated during the activation of zirconocene precatalysts, kinetic investigations were performed following the methodology developed by Bochmann *et al.*¹² NMR spectra were recorded on Bruker AM-

400 and AM-500 spectrometers. ^1H NMR chemical shifts for reaction mixtures were referenced to the residual solvent peaks (CD_2Cl_2). The amount of 1-hexene consumed was monitored over few minutes or hours by ^1H NMR spectroscopy, and signals of monomer were integrated against internal standards (pentamethylbenzene).

The apparent propagation rate constant, k_p^0 , is related to the total amount of precatalyst used in the polymerization reaction. It was deduced from the plot of the amount of polymer as a function of time from which a slope was obtained and introduced in equation (1).

$$\text{Slope} = M_M \times [M]_0 \times C_0 \times k_p^0 \quad (1)$$

where M_M is the molecular weight of the monomer; $[M]_0$ is the initial concentration of monomer, and C_0 is the amount (in mol) of precatalyst used. In order to remain valid, this approach using the method of initial rates requires a constant concentration in monomer, i.e. all the data were acquired under 20% conversion. To determine values of k_p^0 , the parameters $[\text{Zr}]_{\text{tot}} = 0.20 \text{ mmol}\cdot\text{L}^{-1}$, $[\text{MAO}]/[\text{Zr}]_{\text{tot}} = 1000$ and $[1\text{-hexene}]_0/[\text{Zr}]_{\text{tot}} = 8060$ were kept constant.

The standard deviations from the least-squares fit were used to estimate the uncertainties in k_p^0 .³³ The value of the specific rate constant k_p related to the active species was determined with evolution of polymer polymerization degree (DP_n) over time as described by Bochmann and coworkers (equation 2)¹² or a more simple relation reported by Natta (equation 3).³⁴ The optimized algorithm was based on a nonlinear regression analysis using the Levenberg-Marquardt (Damped Least-Squares) method for minimizing function $\langle DP_n \rangle$.³⁵ The corresponding uncertainties for determination of the values of k_p and k_t were derived from the corresponding Jacobian estimated by the Levenberg-Marquardt method.

$$\langle DP_n \rangle = \frac{\frac{(k_p[M]_0 + k_t)t}{k_t} + \frac{k_p[M]_0 + k_t - k_i[M]_0}{k_i[M]_0(k_t - k_i[M]_0)}(e^{-k_i[M]_0 t} - 1) - \frac{k_p[M]_0 \times k_i[M]_0}{k_t^2(k_t - k_i[M]_0)}(e^{-k_t t} - 1)}{t + \frac{1}{k_i[M]_0}e^{-k_i[M]_0 t} - \frac{1}{k_i[M]_0}} \quad (2)$$

$$\langle DP_n \rangle = \frac{k_p[M]_0 t}{1+k_t t} \quad (3)$$

The amount of precatalyst converted into active species can then be estimated from the ratio between k_p^0 and k_p .

Typical monitoring of 1-hexene polymerization reactions. A solution of zirconocene precatalyst (0.010 mmol) in toluene (2.8 mL) was added to an oven-dried Schlenk flask in a glovebox. To the flask, toluene was added (35 mL) under argon and the solution was heated up at the indicated temperature. Then, MAO (2.2 mL of a 30 wt.% solution in toluene, 10 mmol) was added. After the indicated aging time, 1-hexene (10.0 mL, 81 mmol) was added via syringe. The polymerization reaction was kept under magnetic stirring for the indicated time at the indicated temperature and was sampled at regular intervals. The samples (0.5 mL) were injected into vials containing THF–MeOH–HCl (2 mL, 100:1:1 v/v) and pentamethylbenzene (35 mg, 0.24 mmol). Samples for NMR analysis were filtered using wool and analyzed immediately, while samples for GPC measures were evaporated to dry in air overnight and re-dissolved in THF before analysis.

Typical polymerization of 1-hexene with $R_3Al/(C_6F_5)B(OH)_2$ co-activator. A mixture of $(C_6F_5)B(OH)_2$ and AlR_3 , in the desired proportions (in ppm with respect to the precatalyst), was stirred overnight at 60 °C in toluene (35 mL). A solution of dimethyl-metallocene precatalyst (0.010 mmol) in toluene (2.8 mL) was introduced and the resulting mixture was aged for 2 min at 30 °C before the introduction of 1-hexene (10.0 mL, 81 mmol). The polymerization reaction was run over the desired period of time, and the sampling process was identical to that described above in the regular protocol.

Monitoring of 1-hexene polymerization reactions in the presence of ethylene. Upon using the same procedure as that for monitoring homopolymerization of 1-hexene, ethylene (80 mL at standard conditions, ca. 0.1 g) was injected in the polymerization system

using a gas syringe after indicated periods of time. Samples for NMR and GPC analyses were taken and analyzed using the original protocol.

ASSOCIATED CONTENT

Supporting information is available free of charge on the ACS Publications website at DOI: Kinetic plots, NMR data (PDF).

AUTHOR INFORMATION

Corresponding Authors

*E-mail for J.-F.C.: jean-francois.carpentier@univ-rennes1.fr

*E-mail for E.K.: evgueni.kirillov@univ-rennes1.fr

ORCID

Jean-Francois Carpentier: 0000-0002-9160-7662

Evgueni Kirillov: 0000-0002-5067-480X

Notes

The authors declare no competing financial interest.

ACKNOWLEDGEMENTS

This work was supported by Total and Total Research and Technology Feluy (PhD and postdoctoral fellowships to XD and FP, respectively).

REFERENCES

-
- ¹ For a recent review, see: Desert, X.; Carpentier, J.-F.; Kirillov, E. Quantification of active sites in single-site group 4 metal olefin polymerization catalysis. *Coord. Chem. Rev.* **2019**, *386*, 50–68.
- ² (a) Resconi, L.; Fritze, C. in *Polypropylene Handbook* (Ed.: Pasquini, N.), Hanser Publishers, Munich, 2005, pp 107–147. (b) Kaminsky, W. Discovery of Methylaluminoxane as Cocatalyst for Olefin Polymerization. *Macromolecules* **2012**, *45*, 3289–3297. (c) Fink, G.; Brintzinger, H. H. Polymerization Reactions in *Metal-Catalysis in Industrial Organic Processes* (Eds. Chiusoli, G. P.; Maitlis, P. M.), Royal Society of Chemistry, Colchester, 2006, pp 218–254.
- ³ (a) Bochmann, M. The Chemistry of Catalyst Activation: The Case of Group 4 Polymerization Catalysts. *Organometallics* **2010**, *29*, 4711–4740. (b) Bochmann, M. J. Kinetic and mechanistic aspects of metallocene polymerisation catalysts. *Organomet. Chem.* **2004**, *689*, 3982–3998. (c) Pedeutour, J.-N.; Radhakrishnan, K.; Deffieux, A. Reactivity of Metallocene Catalysts for Olefin Polymerization: Influence of Activator Nature and Structure. *Macromol. Rapid Commun.* **2001**, *22*, 1095–1123.
- ⁴ Chen, E. Y.-X.; Marks, T. J. Cocatalysts for Metal-Catalyzed Olefin Polymerization: Activators, Activation Processes, and Structure–Activity Relationships; *Chem. Rev.* **2000**, *100*, 1391–1434.

-
- ⁵ (a) Schnell, D.; Fink, G. Elementarprozesse der Ziegler-Natta-Katalyse. I. Oligomerenkinetik im Strömungsrohr. *Angew. Makromol. Chem.* **1974**, *39*, 131–147. (b) Fink, G.; Zoller, W. Elementarprozesse löslicher ziegler-katalysatoren. Polymerisationskinetische analyse und mathematische modellierung im system $\text{Cp}_2\text{TiPropylCl/AlEtCl}_2/\text{ethylen}$. *Makromol. Chem.* **1981**, *182*, 3265–3278. (c) Fink, G.; Schnell, D. Elementarprozesse der Ziegler-Katalyse. III. Ermittlung der Kettenwachstumsgeschwindigkeitskonstanten aus der Molmassenverteilung. *Angew. Makromol. Chem.* **1982**, *105*, 31–38. (d) Mynott, R.; Fink, G.; Fenzl, W. Ethylene insertion with soluble Ziegler catalysts. III. The system $\text{Cp}_2\text{TiMeCl/AlMe}_2\text{Cl}/^{13}\text{C}_2\text{H}_4$ studied by ^{13}C -NMR spectroscopy. The time-development of chain propagation and oligomer distribution. *Angew. Makromol. Chem.* **1987**, *154*, 1–21. (e) Fink, G.; Fenzl, W.; Mynott, R. Z. Ethylene Insertion with Soluble Ziegler Catalysts: Direct Insight into the Reaction Using Enriched $^{13}\text{C}_2\text{H}_4$ and ^{13}C NMR Spectroscopy II. The System $\text{Cp}_2\text{TiMeCl/AlMeCl}_2/^{13}\text{C}_2\text{H}_4$. *Naturforsch., B* **1985**, *40b*, 158–166.
- ⁶ (a) Keii, T.; Terano, M.; Kimura, K.; Ishii, K. A kinetic argument for a quasi-living polymerization of propene with a MgCl_2 -supported catalyst. *Makromol. Chem., Rapid Commun.* **1987**, *8*, 583–587. (b) Terano, M.; Kataoka, T.; Keii, T. Stopped flow polymerization of propene with typical MgCl_2 -supported high-yield catalysts. *J. Mol. Catal.* **1989**, *56*, 203–210. (c) Terano, M.; Kataoka, T.; Keii, T. Analytical and kinetic approaches for the basic type of MgCl_2 -supported high yield catalysts. *J. Polym. Sci., Part A: Polym. Chem.* **1990**, *28*, 2035–2048.
- ⁷ (a) Shiono, T.; Ohgizawa, M.; Soga, K. Reaction of the Ti-polyethylene bond with carbon monoxide over the bis(cyclopentadienyl)titanium dichloride-methylaluminoxane catalyst system. *Polymer* **1994**, *35*, 187–192. (b) Soga, K.; Ohgizawa, M.; Shiono, T.

-
- Evaluation of propagation rate constants for isotactic and atactic polymerization of propene with MgCl₂-supported catalysts. *Makromol. Chem., Rapid Commun.* **1989**, *10*, 503–507.
- ⁸ (a) Busico, V.; Cipullo, R.; Esposito, V. Stopped-flow polymerizations of ethene and propene in the presence of the catalyst system *rac*-Me₂Si(2-methyl-4-phenyl-1-indenyl)₂ZrCl₂/methylaluminoxane. *Macromol. Rapid Commun.* **1999**, *20*, 116–121. (b) Cipullo, R.; Mellino, S.; Busico, V. Identification and Count of the Active Sites in Olefin Polymerization Catalysis by Oxygen Quench. *Macromol. Chem Phys.* **2014**, *215*, 1728–1734. (c) Cipullo, R.; Melone, P.; Yu, Y.; Iannone, D.; Busico, V. Olefin polymerisation catalysts: when perfection is not enough. *Dalton Trans.* **2015**, *44*, 12304–12311.
- ⁹ (a) Liu, Z.; Somsook, E.; Landis, C. R. A. ²H-Labeling Scheme for Active-Site Counts in Metallocene-Catalyzed Alkene Polymerization. *J. Am. Chem. Soc.* **2001**, *123*, 2915–2916. (b) Liu, Z.; Somsook, E.; White, C. B.; Rosaaen, K. A.; Landis, C. R. Kinetics of Initiation, Propagation, and Termination for the [*rac*-(C₂H₄(1-indenyl)₂)ZrMe][MeB(C₆F₅)₃]-Catalyzed Polymerization of 1-Hexene. *J. Am. Chem. Soc.* **2001**, *123*, 11193–11207.
- ¹⁰ (a) Landis, C. R.; Sillars, D. R.; Batterton, J. M. Reactivity of Secondary Metallocene Alkyls and the Question of Dormant Sites in Catalytic Alkene Polymerization *J. Am. Chem. Soc.* **2004**, *126*, 8890–8891. (b) Sillars, D. R.; Landis, C. R. Catalytic Propene Polymerization: Determination of Propagation, Termination, and Epimerization Kinetics by Direct NMR Observation of the (EBI)Zr(MeB(C₆F₅)₃)propenyl Catalyst Species. *J. Am. Chem. Soc.* **2003**, *125*, 9894–9895. (c) Landis, C. R.; Rosaaen, K. A.; Sillars, D. R. Direct Observation of Insertion Events at *rac*-(C₂H₄(1-indenyl)₂)Zr(MeB(C₆F₅)₃)-Polymeryl Intermediates: Distinction between Continuous

-
- and Intermittent Propagation Modes *J. Am. Chem. Soc.* **2003**, *125*, 1710–1711. (d) Landis, C. R.; Rosaaen, K. A.; Sillars, D. R.; Uddin, J. Heavy-Atom Kinetic Isotope Effects, Cocatalysts, and the Propagation Transition State for Polymerization of 1-Hexene Using the *rac*-(C₂H₄(1-indenyl)₂)ZrMe₂ Catalyst Precursor. *J. Am. Chem. Soc.* **2002**, *124*, 12062–12063. (e) Landis, C. R.; Christianson, M. D. Metallocene-catalyzed alkene polymerization and the observation of Zr-allyls. *Proc. Natl. Acad. Sci. U.S.A.* **2006**, *103*, 15349–15354.
- ¹¹ (a) Christianson, M. D.; Tan, E. H. P.; Landis, C. R. Stopped-Flow NMR: Determining the Kinetics of [*rac*-(C₂H₄(1-indenyl)₂)ZrMe][MeB(C₆F₅)₃]-Catalyzed Polymerization of 1-Hexene by Direct Observation. *J. Am. Chem. Soc.* **2010**, *132*, 11461–11463. (b) Moscato, B. M.; Zhu, B.; Landis, C. R. GPC and ESI-MS Analysis of Labeled Poly(1-Hexene): Rapid Determination of Initiated Site Counts during Catalytic Alkene Polymerization Reactions. *J. Am. Chem. Soc.* **2010**, *132*, 14352–14354. (c) Tan, E. H. P.; Christianson, M. D.; Landis, C. R. Direct kinetic analysis of catalytic alkene polymerization by stopped-flow NMR. *Polymer Preprints* **2011**, *52(1)*, 242–243. (d) Moscato, B. M.; Zhu, B.; Landis, C. R. Mechanistic Investigations into the Behavior of a Labeled Zirconocene Polymerization Catalyst. *Organometallics* **2012**, *32*, 2097–2107. (e) Nelsen, D. L.; Anding, B. J.; Sawicki, J. L.; Christianson, M. D.; Arriola, D. J.; Landis, C. R. Chromophore Quench-Labeling: An Approach to Quantifying Catalyst Speciation As Demonstrated for (EBI)ZrMe₂/B(C₆F₅)₃-Catalyzed Polymerization of 1-Hexene. *ACS Catalysis* **2016**, *6*, 7398–7408. (f) Cueny, E. S.; Johnson, H. C.; Anding, B. J.; Landis, C. R. Mechanistic Studies of Hafnium-Pyridyl Amido-Catalyzed 1-Octene Polymerization and Chain Transfer Using Quench-Labeling Methods. *J. Am. Chem. Soc.* **2017**, *34*, 11903–11912.

-
- ¹² (a) Song, F.; Cannon, R. D.; Bochmann, M. Zirconocene-Catalyzed Propene Polymerization: A Quenched-Flow Kinetic Study. *J. Am. Chem. Soc.* **2003**, *125*, 7641–7653. (b) Song, F.; Cannon, R. D.; Lancaster, S. J.; Bochmann, M. Activator effects in metallocene-based alkene polymerisations: unexpectedly strong dependence of catalyst activity on trityl concentration *J. Mol. Catal. A: Chem.* **2004**, *218*, 21–28. (c) Song, F.; Cannon, R. D.; Bochmann, M. The kinetics of propene and hexene polymerisation with [(SBI)ZrR]₂X⁻: evidence for monomer-dependent early or late transition states. *Chem. Commun.* **2004**, 542–543. (d) Ghiotto, F.; Pateraki, C.; Severn, J. R.; Friederichs, N.; Bochmann, M. Rapid evaluation of catalysts and MAO activators by kinetics: what controls polymer molecular weight and activity in metallocene/MAO catalysts?. *Dalton Trans.* **2013**, *42*, 9040–9048.
- ¹³ Novstrup, K. A.; Travia, N. E.; Medvedev, G. A.; Stanciu, C.; Switzer, J. M.; Thomson, K. T.; Delgass, W. N.; Abu-Omar, M. M.; Caruthers, J. M. Mechanistic Detail Revealed via Comprehensive Kinetic Modeling of [rac-C₂H₄(1-indenyl)₂ZrMe₂]-Catalyzed 1-Hexene Polymerization. *J. Am. Chem. Soc.* **2010**, *132*, 558–566.
- ¹⁴ Chen, C. H.; Shih, W. C.; Hilty, C. In Situ Determination of Tacticity, Deactivation, and Kinetics in [rac-(C₂H₄(1-Indenyl)₂ZrMe][B(C₆F₅)₄] and [Cp₂ZrMe][B(C₆F₅)₄]-Catalyzed Polymerization of 1-Hexene Using ¹³C Hyperpolarized NMR. *J. Am. Chem. Soc.* **2015**, *137*, 6965–6971.
- ¹⁵ Guo, Y.; He, F.; Zhang, Z.; Khan, A.; Fu, Z.; Xu, J.; Fan, Z. Influence of trimethylaluminum on kinetics of rac-Et(Ind)₂ZrCl₂/aluminoxane catalyzed ethylene polymerization. *J. Organomet. Chem.* **2016**, *808*, 109–116.
- ¹⁶ Spaleck, W.; Kuber, F.; Winter, A.; Rohrmann, J.; Bachmann, B.; Antberg, M.; Dolle, V.; Paulus, E. F. The Influence of Aromatic Substituents on the Polymerization Behavior of Bridged Zirconocene Catalyst. *Organometallics* **1994**, *13*, 954–963.

- ¹⁷ (a) Kirillov, E.; Marquet, N.; Razavi, A.; Belia, V.; Hampel, F.; Roisnel, T.; Gladysz, J. A.; Carpentier, J.-F. New C₁-Symmetric Ph₂C-Bridged Multisubstituted ansa-Zirconocenes for Highly Isospecific Propylene Polymerization: Synthetic Approach via Activated Fulvenes. *Organometallics* **2010**, *29*, 5073–5082. (b) Kirillov, E.; Marquet, N.; Bader, M.; Razavi, A.; Belia, V.; Hampel, F.; Roisnel, T.; Gladysz, J. A.; Carpentier, J.-F. Chiral-at-ansa-Bridged Group 4 Metallocene Complexes {(R¹R²C)-(3,6-tBu₂Flu)(3-R³-5-Me-C₅H₂)}MCl₂: Synthesis, Structure, Stereochemistry, and Use in Highly Ioselective Propylene Polymerization *Organometallics* **2011**, *30*, 263–272. (c) Bader, M.; Marquet, N.; Kirillov, E.; Roisnel, T.; Razavi, A.; Lhost, O.; Carpentier, J.-F. Old and New C₁-Symmetric Group 4 Metallocenes {(R¹R²C)-(R²R³R⁶R⁷-Flu)(3-R₃-5-R⁴-C₅H₂)}ZrCl₂: From Highly Isotactic Polypropylenes to Vinyl End-Capped Isotactic-Enriched Oligomers. *Organometallics* **2013**, *32*, 8375–8387. (d) Castro, L.; Kirillov, E.; Miserque, O.; Welle, A.; Haspelslagh, L.; Carpentier, J.-F.; Maron, L. Are Solvent and Dispersion Effects Crucial in Olefin Polymerization DFT Calculations? Some Insights from Propylene Coordination and Insertion Reactions with Group 3 and 4 Metallocenes. *ACS Catal.* **2015**, *5*, 416–425.
- ¹⁸ (a) Kim, I.; Zhou, J.-M.; Chung, H. Higher α -Olefin Polymerizations Catalyzed by *rac*-Me₂Si(1-C₅H₂-2-CH₃-4-tBu)₂Zr(NMe₂)₂/Al(iBu)₃/[Ph₃C][B(C₆F₅)₄]. *J. Polym. Sci. Part A: Polym. Chem.* **2000**, *38*, 1687–1697. (b) Grumel, V.; Brull, R.; Pasch, H.; Raubenheimer, H. G.; Sanderson, R.; Wahner, U. M. Homopolymerization of Higher 1-Olefins with Metallocene/MAO Catalysts. *Macromol. Mater. Eng.* **2001**, *286*, 480–487. (c) Kawahara, N.; Saito, J.; Matsuo, S.; Kaneko, H.; Matsugi, T.; Toda, Y.; Kashiva, N. Study on Unsaturated Structures of Polyhexene, poly(4-methylpentene) and poly(3-methylpentene) Prepared with Metallocene Catalysts. *Polymer* **2007**, *48*, 425–428. (d) Brant, P.; Jiang, P.; Lovell, J.; Crowther, D. Termination Events in Sterically Hindered

-
- Metallocene-Catalyzed Olefin Oligomerizations: Vinyl Chain Ends in Oligooctenes. *Organometallics* **2016**, *35*, 2836–2839. (e) Nifant'ev, I. E.; Vinogradov, A. A.; Vinogradov, A. A.; Churakov, A. V.; Bagrov, V. V.; Kashulin, I. A.; Roznyatovsky, V. A.; Grishin, Y. K.; Ivchenko, P. V. Catalytic Behavior of Heterocenes Activated by TIBA and MMAO Under a Low Al/Zr Ratios in 1-Octene Polymerization. *Appl. Cat. A, Gen.* **2019**, *571*, 12–24.
- ¹⁹ (a) Richter, B.; Meetsma, A.; Hessen, B.; Teuben, J. H. Structural Characterization of a Cationic Zirconocene Olefin Polymerization Catalyst with its Methylated Boralumoxane Counterion. *Angew. Chem. Int. Ed.* **2002**, *41*, 2166–2169. (b) Richter, B.; Gregorius, H. Process for the preparation of catalyst paste and products thereof. *Int. Pat. WO 2009043867*, **2009**. (c) Richter, B.; Gregorius, H. Methods of preparing metallocene catalysts. *Int. Pat. WO 2012080294*, **2012**.
- ²⁰ Tanaka, R.; Hirose, T.; Nakayama, Y.; Shiono, T. The preparation of boron-containing aluminoxanes and their application as cocatalysts in the polymerization of olefins. *Polym. J.*, **2016**, *48*, 67–71.
- ²¹ (a) Babushkin, D. E.; Panchenko, V. N.; Brintzinger, H.H. Zirconium Allyl Complexes as Participants in Zirconocene-Catalyzed α -Olefin Polymerizations. *Angew. Chem. Int. Ed.* **2014**, *53*, 9645–9649. (b) Panchenko, V. N.; Babushkin, D. E.; Brintzinger, H.H. Zirconium-Allyl Complexes as Resting States in Zirconocene-Catalyzed α -Olefin Polymerization. *Macromol. Rapid Commun.* **2015**, *36*, 249–253.
- ²² Vatamanu, M. Observation of zirconium allyl species formed during zirconocene-catalyzed propene polymerization and mechanistic insights. *J. Catal.* **2015**, *323*, 112–120.
- ²³ (a) Corradini, P.; Busico, V.; Cipullo, R. Hydroooligomerization of propene: a “fingerprint” of a Ziegler-Natta catalyst, 2. A reinterpretation of results for isospecific

-
- homogeneous systems. *Macromol. Chem., Rapid Commun.* **1992**, *13*, 21–24. (b)
- Busico, V.; Cipullo, R.; Corradini, P. Preliminary results of propene hydroooligomerization in the presence of the homogeneous isospecific catalyst system *rac*-(EBI)ZrCl₂/MAO. *Macromol. Chem., Rapid Commun.* **1993**, *14*, 97–103.
- ²⁴ Busico, V.; Cipullo, R.; Pellecchia, R.; Talarico, G.; Razavi, A. Hafnocenes and MAO: Beware of Trimethylaluminum!. *Macromolecules* **2009**, *42*, 1789–1791.
- ²⁵ Theurkauff, G.; Bader, M.; Marquet, N.; Bondon, A.; Roisnel, T.; Guegan, J.-P.; Amar, A.; Boucekkine, A.; Carpentier, J.-F.; Kirillov, E. Discrete Ionic Complexes of Highly Isoselective Zirconocenes. Solution Dynamics, Trimethylaluminum Adducts, and Implications in Propylene Polymerization. *Organometallics* **2016**, *35*, 258–276.
- ²⁶ Yu, Y.; Busico, V.; Budzelaar, P. H. M.; Vittoria, A.; Cipullo, R. Of Poisons and Antidotes in Polypropylene Catalysis. *Angew. Chem. Int. Ed.* **2016**, *55*, 8590–8594.
- ²⁷ The possible concomitant hydrogenation of 1-hexene can also account for the observed lower polymer yield, see: Cui, X.; Burgess, K. Catalytic Homogeneous Asymmetric Hydrogenations of Largely Unfunctionalized Alkenes. *Chem. Rev.* **2005**, *105*, 3272–3296.
- ²⁸ (a) Busico, V.; Cipullo, R.; Talarico, G. Highly Regioselective Transition-Metal-Catalyzed 1-Alkene Polymerizations: A Simple Method for the Detection and Precise Determination of Regioirregular Monomer Enchainments. *Macromolecules* **1998**, *31*, 2387–2390. (b) Busico, V.; Cipullo, R.; Talarico, G. Propene/Ethene-[1-¹³C] Copolymerization as a Tool for Investigating Catalyst Regioselectivity. 1. Theory and Calibration. *Macromolecules* **2002**, *35*, 1537–1542.
- ²⁹ Lin, S.; Waymouth, R. M. 2-Arylindene Metallocenes: Conformationally Dynamic Catalysts To Control the Structure and Properties of Polypropylenes. *Macromolecules* **1999**, *32*, 8283–8290.

-
- ³⁰ Resconi, L.; Camurati, I.; Sudmeijer, O. Chain transfer reactions in propylene polymerization with zirconocene catalysts. *Topics in Catalysis* **1999**, *7*, 145–163.
- ³¹ The olefinic region of the $^{13}\text{C}\{^1\text{H}\}$ NMR spectrum of the copolymer obtained with **{SBI}-2** showed only a minute resonance assigned to terminal vinylidene end-groups (δ 111.6 ppm; Fig. S22), which result from regular β -H elimination reaction; all other end-groups were saturated (alkyls). Also, only saturated end-groups were observed in poly(propylene-*co*-ethylene) copolymers produced by **{Cp/Flu}-1**.
- ³² Razavi, A. *PCT Int. Appl.* **1999**, WO00/49029 (to Atofina Co.).
- ³³ (a) Bevington, P. R. *Data Reduction and Error Analysis for the Physical Sciences*; McGraw-Hill: New York, 1969. (b) Skoog, D. A.; Leary, J. J. *Principles of Instrumental Analysis*, 4th ed.; Saunders College: Fort Worth, TX, 1992; pp 13–14.
- ³⁴ Natta, G.; Pasquon, I. The Kinetics of the Stereospecific Polymerization of α -Olefins. *Adv. Catal.* **1959**, *11*, 1–66.
- ³⁵ Constantinides, A.; Mostoufi, N. *Numerical Methods for Chemical Engineers with MATLAB Applications*, Prentice Hall, Upper Saddle River, NJ, USA, 1999.